Atom insertion into grain boundaries and stress generation in physically vapor deposited films

Daniel Magnfält, G Abadias and Kostas Sarakinos

Original Publication:

Daniel Magnfält, G Abadias and Kostas Sarakinos, Atom insertion into grain boundaries and stress generation in physically vapor deposited films, 2013, Applied Physics Letters, (103), 5.
http://dx.doi.org/10.1063/1.4817669

Atom insertion into grain boundaries and stress generation in physically vapor deposited films

D. Magnfält,[1,a)] G. Abadias,[2] and K. Sarakinos[1]
[1]*Plasma and Coatings Physics Division, Department of Physics, Chemistry and Biology (IFM), Linköping University, SE-58183 Linköping, Sweden*
[2]*Institut P', Département Physique et Mécanique des Matériaux, Université de Poitiers-CNRS-ENSMA, SP2MI, Téléport 2, Bd M. et P. Curie, F-86962 Chasseneuil-Futuroscope, France*

(Received 16 May 2013; accepted 19 July 2013; published online 2 August 2013)

We present evidence for compressive stress generation via atom insertion into grain boundaries in polycrystalline Mo thin films deposited using energetic vapor fluxes (<∼120 eV). Intrinsic stress magnitudes between −3 and +0.2 GPa are obtained with a nearly constant stress-free lattice parameter marginally larger (0.12%) than that of bulk Mo. This, together with a correlation between large compressive film stresses and high film densities, implies that the compressive stress is not caused by defect creation in the grains but by grain boundary densification. Two mechanisms for diffusion of atoms into grain boundaries and grain boundary densification are suggested. © *2013 AIP Publishing LLC*. [http://dx.doi.org/10.1063/1.4817669]

Intrinsic stresses are crucial for film functionality, since they largely determine film adhesion on underlying substrates, while they have implications for mechanical and optical properties of films.[1–3] The origin and evolution of intrinsic stresses in physical vapor deposited polycrystalline films have been thoroughly investigated during the past decades,[1,3,4] highlighting the role of grain boundaries for stress generation.[5–11] Films deposited at homologous temperatures, T_s/T_m, well below 0.2 tend to be in a tensile stress state due to attraction between neighboring grains over underdense grain boundaries,[5,6] formed as a result of the limited mobility of film forming species (adatoms) at these conditions.[12] On the other hand, when deposition is performed at relatively high T_s/T_m (typically above 0.2), adatoms have sufficient mobility for dense films to form,[12] which is accompanied by generation of a compressive growth stress after formation of a continuous film.[1,4,10] This phenomenon has been explained based on results from *in situ* monitoring of intrinsic stress evolution during and after deposition, growth simulations, and analytical models[8,9,13–17] to be the effect of diffusion of adatoms into grain boundaries driven by a chemical potential difference between the latter and the film surface.[8,9] However, direct experimental evidence for insertion of film forming species into grain boundaries is not available in the literature, since this would require observation of atoms exiting grain boundaries after deposition is ceased. Instead, indirect evidence can be sought by studying the microstructural evolution during growth. However, the fast dynamics of thin film growth make *in situ* and/or post-growth correlation between film microstructural evolution, atom diffusion, and stress generation a non-trivial task. For instance, at high T_s/T_m, post-deposition and out-diffusion of atoms from supersaturated grain boundaries[8,9] and microstructural reorganization[11] have both been suggested to contribute to compressive stress relaxation. A way to circumvent these limitations and seek evidence for insertion of film forming species into grain boundaries is to establish the relationships between film stress state and microstructure by freezing the state of the film at the completion of deposition. This can be achieved by employing growth conditions that facilitate sufficient atomic mobility on the surface and in near-surface layers during deposition but result in negligible post-deposition surface and bulk mobility. These growth conditions can be encountered when depositing films at relatively low T_s/T_m under concurrent bombardment by large fluxes of hyperthermal species, with energies of the order of several 10s up to ∼100 eV, which only influence the first few atomic layers of the film.[12] In the present study, this strategy is implemented by growing Mo films using highly ionized energetic fluxes generated by a high power impulse magnetron sputtering (HiPIMS) discharge.[18–22] Our results contribute to the understanding of intrinsic stresses in polycrystalline films by providing further evidence for compressive stress generation via insertion of film forming species into grain boundaries. We also suggest two concurrent energetic bombardment induced mechanisms for diffusion of atoms into grain boundaries.

The HiPIMS discharge was operated at peak target powers, P_{Tp}, between 4.5 and 152 kW, seeking to alter the energy and the flux of the ionized species impinging onto the growing film.[19,20] This was achieved by using 50 μs wide voltage pulses with frequencies ranging from 100 to 1000 Hz at two different working pressures, 0.16 and 0.40 Pa. The energies and fluxes of Ar^+, Mo^+, Ar^{2+}, and Mo^{2+} ions were measured using time- and energy-resolved ion mass spectrometry.[23] From the ion energy distribution functions (IEDFs) in Fig. 1, it can be seen that Ar^+ ions (Fig. 1(a)) exhibit considerable fluxes up to energies of ∼10 eV, and they are therefore less energetic than the other ionized species that exhibit IEDFs extending up to maximum ∼120 eV. Furthermore, Fig. 1 shows that an increase of P_{Tp} leads to broader IEDFs and higher ion intensities for all species. Other energetic species in magnetron sputtering processes are sputtered (Mo) atoms and gas (Ar) atoms backscattered from the target surface. The generation, gas transport, and energies of these species when impinging on the substrate

a)Author to whom correspondence should be addressed. Electronic mail: danma@ifm.liu.se

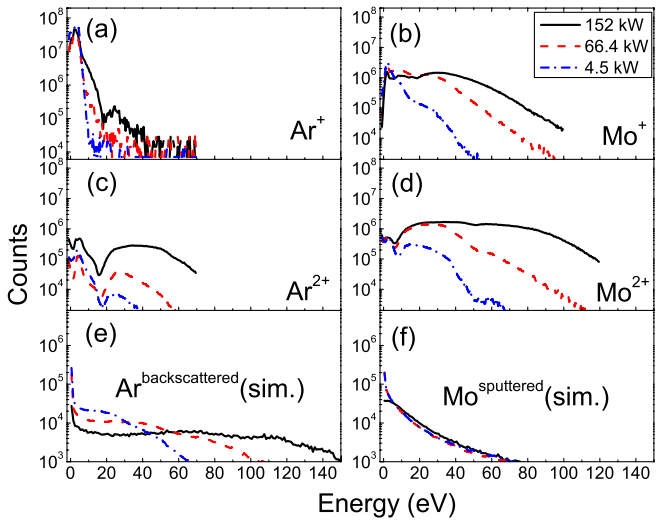

FIG. 1. Energy distribution functions of (a) Ar^+, (b) Mo^+, (c) Ar^{2+}, and (d) Mo^{2+} ions measured by time-averaged mass spectrometry measurements, (e) backscattered Ar atoms, and (f) sputtered Mo atoms estimated by Monte-Carlo based (TRIM and SIMTRA) simulations, at different P_{TP}.

were simulated using the TRIM[24] and SIMTRA[25] codes. The simulations showed that the energy of Ar atoms backscattered from the target surface is affected by the deposition conditions (Fig. 1(e)) while the energy distributions of sputtered Mo atoms (Fig. 1(f)) are similar for all process conditions.

Mo films with thickness between 50 and 150 nm were deposited at the process conditions given in the previous paragraph onto electrically floating Si (100) substrates covered with native oxide. No intentional substrate heating was used, and the homologous temperature T_s/T_m was thus estimated to be below 0.13. X-ray diffractometry showed that all films had a strong (110) out-of-plane preferred orientation and a weak in-plane orientation.[23] The effect of the deposition conditions on the intrinsic stress (σ) and the stress-free lattice parameter (a_0) was studied using the crystallite group method[26] and the $\sin^2\psi$ method adapted for textured layers.[23] Fig. 2(a) shows that σ takes values from +0.2 to −3 GPa

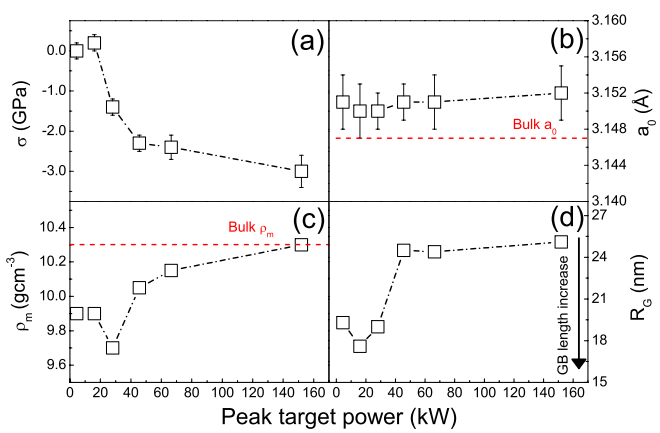

FIG. 2. Effect of the peak target power on (a) biaxial stress (σ), (b) stress-free lattice parameter (a_0), (c) film mass density (ρ_m), and (d) grain radius (R_G). The grain boundary (GB) length scales inversely with the grain radius as indicated by the solid arrow in (d). The horizontal dashed lines in (b) and (c) indicate the stress-free bulk lattice parameter and the bulk mass density for Mo, respectively.

with larger energies and fluxes of bombarding species (corresponding to larger P_{Tp} values) resulting in larger compressive stresses. Despite the differences in the stress sign and magnitude, P_{Tp} variations do not significantly affect a_0 which has a mean value of $\sim 3.151 \pm 0.001$ Å (Fig. 2(b)); this value is only marginally larger (0.12%) than the stress-free lattice parameter of bulk Mo (3.147 Å)[27] indicated by the horizontal dashed line in Fig. 2(b). For polycrystalline films deposited under energetic bombardment it is well established in the literature[28–31] that compressive stresses result from implantation of bombarding gas species into the grains or from point defects generated in the collision cascades induced by bombarding species. Both these mechanisms cause a hydrostatic expansion of the lattice that manifests itself as an expansion of the stress-free lattice parameter. For instance, Debelle *et al.*[28] measured compressive stresses of 4 GPa accompanied by stress-free lattice parameters up to 3.165 Å in Mo films deposited using ion beam sputtering with 1.2 keV Ar^+ ions impinging onto the Mo target. The stress-free lattice parameter was calculated to correspond to a hydrostatic compressive stress component of approximately 3 GPa.[28] The small and nearly constant expansion of the stress-free lattice parameter in the present study implies that the hydrostatic stress component is small and nearly the same for all films. Therefore the differences in stress sign and magnitude between the films cannot be attributed to changes in defect concentration in the grains. Instead the compressive stress is mainly *biaxial*.

A mechanism that can lead to generation of biaxial compressive stresses is insertion of atoms into grain boundaries.[8,9,15,16] However, the limited mobility under the conditions used in the present work ($T_s/T_m \sim 0.13$) often leads to underdense grain boundaries that result in low film mass densities.[12] The mass density (ρ_m) of the films was investigated using X-ray reflectometry[23] which showed (results presented in Fig. 2(c)) that conditions that favor large compressive stress magnitudes also lead to ρ_m values close to that of bulk Mo (10.3 g/cm^3, indicated by the dashed horizontal line in Fig. 2(c)). The decrease in the compressive stress magnitude is accompanied by a decrease in the mass density, resulting in film densities ~5% smaller than the density of bulk Mo for films in the tensile stress regime. The total mass density of the film depends on the mass density of the grain boundary regions and the grain boundary length. The latter scales as the inverse of the in-plane grain size. The in-plane grain radii, R_G, of the films were determined using atomic force microscopy[23] (Fig. 2(d)) which showed that a P_{Tp} above ~60 kW results in mean R_G, between 24 and 25 nm decreasing to 18–19 nm for P_{Tp} below ~60 kW. In other words, an increase of P_{Tp} leads to a decrease of the grain boundary length. This may partially account for the film mass density variations observed in Fig. 2(c) as the film density is inversely proportional to the grain boundary length, i.e., it scales with R_G, for underdense grain boundaries. Tensile stresses are generated due to attraction between grains over underdense grain boundaries and are additive with the hydrostatic compressive stresses generated by point defects in the grain bulk.[31] The tensile stress magnitude is proportional to the grain boundary length and could therefore explain the decrease of the compressive stress magnitude

with decreasing peak power in Fig. 2(a). This however would imply that the large compressive stresses generated for large peak target powers are due to point defect incorporation in the grains. This is not the case according to the results presented in Figs. 2(a) and 2(b). Thus, it is possible to conclude that the film density increase with increasing P_{TP} is primarily due to grain boundary densification and that the observed compressive stresses largely are a consequence of this densification.

Insertion of film forming species into grain boundaries as a cause for compressive stresses has been suggested by Chason *et al.*,[8,9] who developed a model that accounts for thermal diffusion of adatoms into grain boundaries at conditions of sufficient surface mobility. In the present study, the growth conditions employed yield a T_s/T_m of the order of 0.13, imposing kinetic constraints on surface diffusion. Energetic bombardment can, however, induce surface diffusion. Growth simulations of Pt on Pt(111) using hyperthermal ($E_{kin} < 50$ eV) Pt atoms[32] have shown that energetic bombardment results in increased rates of intra- and interlayer transport due to momentum transfer to atoms close to the impact site. Therefore, we suggest that bombardment by energetic Mo and Ar species with energies up to 120 eV (Fig. 1) enhances adatom diffusion which, in the proximity of grain boundaries, leads to adatom diffusion into the junction at the top of the grain boundaries (Fig. 3), resembling the thermal diffusion process described in the model by Chason *et al.*[8,9] Bombarding species with energies from several 10s up to 100 eV are also known to affect the subsurface film layers. Monte-Carlo simulations (using TRIM) were used to assess the interaction of Mo and Ar species with energies between 10 and 100 eV with Mo atomic ensembles. The results showed that by increasing energy from 10 to 100 eV the implantation depth of the bombarding species in Mo increases from 2 to 6 Å, corresponding to 1–3 monolayers in Mo (110). Shallow implantation of bombarding species is known to cause generation of point defects, i.e., interstitials, vacancies, and substitutional atoms.[28] Interstitials and substitutional atoms are, in general, unstable and can be annihilated by diffusion towards the nearest underdense region if sufficient energy is provided, e.g., by ion irradiation.[28] For instance, Mo self-interstitials have a positive energy of formation of ~7.3 eV/atom[33] and an activation energy for diffusion of ~0.05 eV.[33,34] We suggest that the shallowly implanted hyperthermal Mo and Ar species transfer a sufficient part of their energy to trigger diffusion of interstitial atoms (Mo and Ar) towards underdense regions, i.e., the surface of the growing film and vacancy-rich regions, but also towards grain boundaries for interstitials located in their vicinity (Fig. 3). By increasing the flux of energetic depositing species and/or their energy (facilitated by increasing P_{Tp} as shown in Fig. 1), surface and subsurface diffusion lengths increase resulting in larger effective acceptance widths for insertion of atoms into the grain boundary and generation of compressive stress. Only a small fraction of the point defects is trapped in the film lattice causing the slight out-of-plane lattice expansion that is observed in Fig. 2(c). This is in contrast to what is observed at growth conditions where the majority of film forming species has a low energy (less than a few eV), and bombardment is provided by Ar species of relatively high energies and low fluxes.[12] In the latter case Ar atoms are implanted at larger depths and trapped in the film before diffusion can be activated by collision cascades generated by other impinging energetic species.[28] Direct implantation of metal and gas species in the grain boundaries, although favored from an energy point of view since the grain boundaries may exhibit a lower density than the grains and thus a smaller implantation threshold, is a rather improbable scenario owing to the much smaller projected area of the grain boundaries as compared to that of the grains (Fig. 3).

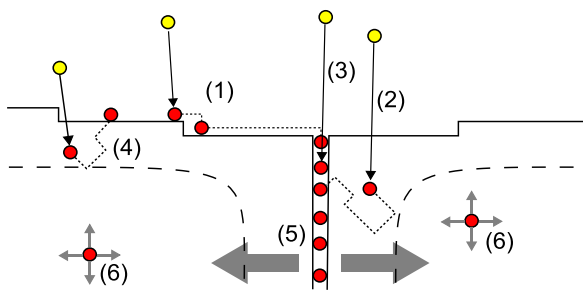

FIG. 3. Schematic view of pathways for atom insertion into grain boundaries through surface diffusion (1), point defect generation via direct or knock-on implantation in the grain and defect diffusion to the grain boundary (2), and direct implantation (3) in the unlikely event of energetic depositing species directly impinging on the grain boundary. The energetic depositing species affect the first few atomic layers (delimited by the dashed lines) enhancing the diffusivity of point defects either to the grain boundary (2) or the surface (4). Atoms in the grain boundaries generate biaxial stress fields in the grains (5) while in-grown point defects generate triaxial stress fields (6).

In summary, we have shown that Mo films can be grown with stresses in the range −3 to 0.2 GPa, depending on the energy of the deposition flux. Despite the differences in the stress sign and magnitude, the stress-free lattice parameter is nearly constant for all deposition conditions and only slightly expanded from the bulk lattice parameter of Mo. This together with a correlation between the compressive stress magnitude and film density provides evidence that the compressive stress is generated through grain boundaries densification. We suggest that the latter is driven by energetic bombardment enhanced surface and subsurface diffusion of deposited species into the grain boundaries.

G.A. acknowledges the support from COST Action MP0804 "Highly Ionized Pulsed Plasmas" that has financed the short-term scientific mission (STSM) at Linköping University during which part of this work was performed. K.S. acknowledges financial support from Linköping University through the "LiU Research Fellows" program. The authors gratefully acknowledge Professor Ulf Helmersson for helpful discussions and input on the manuscript and also Professor Ivan Petrov and Professor Joe Greene for helpful discussions.

[1]R. Koch, Surf. Coat. Technol. **204**, 1973 (2010).
[2]D. Sander, J. Phys.: Condens. Matter **16**, R603 (2004).
[3]G. C. A. M. Janssen, Thin Solid Films **515**, 6654 (2007).
[4]J. A. Floro, E. Chason, R. C. Cammarata, and D. J. Srolovitz, MRS Bull. **27**, 19 (2002).
[5]R. W. Hoffman, Thin Solid Films **34**, 185 (1976).
[6]G. C. A. M. Janssen, A. J. Dammers, V. G. M. Sivel, and W. R. Wang, Appl. Phys. Lett. **83**, 3287 (2003).

[7]B. W. Sheldon, A. Bhandari, A. F. Bower, S. Raghavan, X. Weng, and J. M. Redwing, Acta Mater. **55**, 4973 (2007).
[8]E. Chason, J. W. Shin, S. J. Hearne, and L. B. Freund, J. Appl. Phys. **111**, 083520 (2012).
[9]E. Chason, Thin Solid Films **526**, 1 (2012).
[10]D. Flötotto, Z. M. Wang, L. P. H. Jeurgens, E. Bischoff, and E. J. Mittemeijer, J. Appl. Phys. **112**, 043503 (2012).
[11]A. González-González, C. Polop, and E. Vasco, Phys. Rev. Lett. **110**, 056101 (2013).
[12]I. Petrov, P. B. Barna, L. Hultman, and J. E. Greene, J. Vac. Sci. Technol. A **21**, S117 (2003).
[13]J. S. Tello, A. F. Bower, E. Chason, and B. W. Sheldon, Phys. Rev. Lett. **98**, 216104 (2007).
[14]C. Pao, S. M. Foiles, E. B. Webb, D. J. Srolovitz, and J. A. Floro, Phys. Rev. B **79**, 224113 (2009).
[15]R. Daniel, K. J. Martinschitz, J. Keckes, and C. Mitterer, Acta Mater. **58**, 2621 (2010).
[16]L. E. Kousokeras and G. Abadias, J. Appl. Phys. **111**, 093509 (2012).
[17]J. Leib, R. Mönig, and C. V. Thompson, Phys. Rev. Lett. **102**, 256101 (2009).
[18]V. Kouznetsov, K. Macak, J. M. Schneider, U. Helmersson, and I. Petrov, Surf. Coat. Technol. **122**, 290 (1999).
[19]U. Helmersson, M. Lattemann, J. Böhlmark, A. P. Ehiasarian, and J. T. Gudmundsson, Thin Solid Films **513**, 1 (2006).
[20]K. Sarakinos, J. Alami, and S. Konstantinidis, Surf. Coat. Technol. **204**, 1661 (2010).
[21]J. Böhlmark, M. Lattemann, J. T. Gudmundsson, A. P. Ehiasarian, Y. A. Gonzalvo, N. Brenning, and U. Helmersson, Thin Solid Films **515**, 1522 (2006).
[22]A. Hecimovic and A. P. Ehiasarian, IEEE Trans. Plasma Sci. **39**, 1154 (2011).
[23]See supplementary material at http://dx.doi.org/10.1063/1.4817669 for specific information on the experimental procedures and additional AFM, XRR, and XRD data.
[24]J. F. Ziegler, J. P. Biersack, and U. Littmark, *The Stopping and Range of Ions in Solids* (Pergamon, New York, 1985).
[25]K. Van Aeken, S. Mahieu, and D. Depla, J. Phys. D: Appl. Phys. **41**, 205307 (2008).
[26]V. Hauk, W. K. Krug, R. W. M. Oudelhoven, and L. Pintschovius, Z. Metallk. **79**, 159 (1988).
[27]JCPDS Card No. 42–1120.
[28]A. Debelle, G. Abadias, A. Michel, C. Jaouen, and V. Pelosin, J. Vac. Sci. Technol. A **25**, 1438 (2007).
[29]J.-D. Kamminga, Th. H. de Keijser, R. Delhez, and E. J. Mittemeijer, J. Appl. Phys. **88**, 6332 (2000).
[30]G. Abadias and Y. Y. Tse, J. Appl. Phys. **95**, 2414 (2004).
[31]G. C. A. M. Janssen and J.-D. Kamminga, Appl. Phys. Lett. **85**, 3086 (2004).
[32]D. Adamovic, V. Chirita, E. P. Münger, L. Hultman, and J. E. Greene, Phys. Rev. B **76**, 115418 (2007).
[33]S. Han, L. A. Zepeda-Ruiz, G. J. Ackland, R. Car, and D. J. Srolovitz, Phys. Rev. B **66**, 220101(R) (2002).
[34]F. W. Young, Jr., J. Nucl. Mater. **69/70**, 310 (1978).